

Effect of Hydrate on the Deliverability of Underground Gas Storage (UGS) Reservoir

Charlie Iyke C. Anyadiegwu, Christian Emelu Okalla*, Anthony Kerunwa, Nmesoma Precious Ebosie, Daniel Chinedu Nwachukwu, Federal University of Technology Owerri, Owerri, Nigeria

Abstract

The study investigates the impact of hydrates on the deliverability of underground gas storage (UGS) reservoirs, specifically focusing on depleted wells. Utilizing MATLAB (2024) for numerical problem coding and Microsoft Office Excel (2013) for data collation and plotting, the research simulates the effects of hydrate formation within a gas well. Data was sourced from open literature and includes parameters such as gas gravity, tubing dimensions, pressures, temperatures, and constants for the inflow performance relationship (IPR) model. Key metrics, such as gas gravity, tubing inside diameter, and reservoir pressure, were used to model the gas storage well's behavior. The study varied the hydrate film thickness from 0.0 to 1.0 inch to assess its influence on gas deliverability. The governing equations for IPR and tubing performance relationship (TPR) were employed, integrating the hydrate film's impact by modifying the inner diameter of the tubing. The IPR equation was rearranged to compute the flowing bottom-hole pressure as a function of flow rate. The TPR equation was adjusted to account for hydrate thickness, leading to a new model that predicts gas deliverability under varying hydrate conditions. The solution procedure involved computing average temperature and pressure, critical temperature and pressure, pseudo-reduced temperature and pressure, and average compressibility factor. These computations facilitated the generation of gas flow rates and the plotting of IPR and TPR curves for different hydrate thicknesses. Results indicated that as hydrate film thickness increases, the TPR curve shifts from horizontal to vertical, signifying reduced gas flow rates and increased bottom-hole pressures. A hydrate thickness of 0.0 inches resulted in a flow rate of 1470 Mscf/day, while a thickness of 1.0 inch reduced the flow rate to 20 Mscf/day. This reduction in flow rate and increase in bottom-hole pressure illustrate the adverse effects of hydrate deposition on gas well deliverability. In conclusion, the presence of hydrates significantly decreases the deliverability of gas storage wells. To mitigate these effects, the study recommends the use of hydrate inhibitors and insulation of pipelines to prevent heat loss, thereby avoiding hydrate formation.

Introduction

Natural gas plays a pivotal role in meeting global energy demands, and underground gas storage (UGS) reservoirs are essential for ensuring a stable and reliable supply of natural gas to consumers. Depleted wells, characterized by lower reservoir pressures, are commonly repurposed for UGS operations due to their existing infrastructure (Chu et al. 2023). However, the presence of hydrates in such reservoirs poses a significant challenge to the deliverability and overall efficiency of these storage facilities (Muhammed et al. 2023). Hydrates are solid compounds formed by the combination of water and natural gas molecules under specific temperature and pressure conditions (Wang and Economides 2009). In UGS reservoirs in depleted wells, the potential for hydrate formation is heightened due to the reduced reservoir pressures and temperatures commonly associated with these

Copyright © the author(s). This work is licensed under a Creative Commons Attribution 4.0 International License.

Improved Oil and Gas Recovery

DOI: 10.14800/IOGR.1313

Received September 14, 2024; revised September 22, 2024; accepted October 8, 2024.

*Corresponding author: christian.okalla@futo.edu.ng

conditions. The formation of hydrates can have several adverse effects on reservoir performance, with a direct impact on deliverability.

As natural gas is injected into depleted wells during periods of excess supply and withdrawn during periods of high demand, the thermodynamic and kinetic factors influencing hydrate stability become critical. Hydrate formation can lead to reduced permeability within the reservoir rock and near the wellbore, creating flow restrictions that impede the movement of natural gas (Dillon 2002). This restriction in flow can result in a decline in well deliverability, making it essential to understand and address the hydrate-related challenges specific to UGS operations in depleted wells. To assess and manage the impact of hydrates on UGS reservoir deliverability, it is crucial to delve into the underlying mechanisms of hydrate formation, considering both thermodynamic and kinetic aspects. Thermodynamically, hydrates are stable under specific pressure and temperature conditions, and these conditions are often encountered in depleted wells. Kinetic considerations involve understanding the rate at which hydrates form and dissolve, which is essential for predicting and mitigating hydrate-related issues during injection and withdrawal cycles. **Figure 1** highlights the purpose of USS.

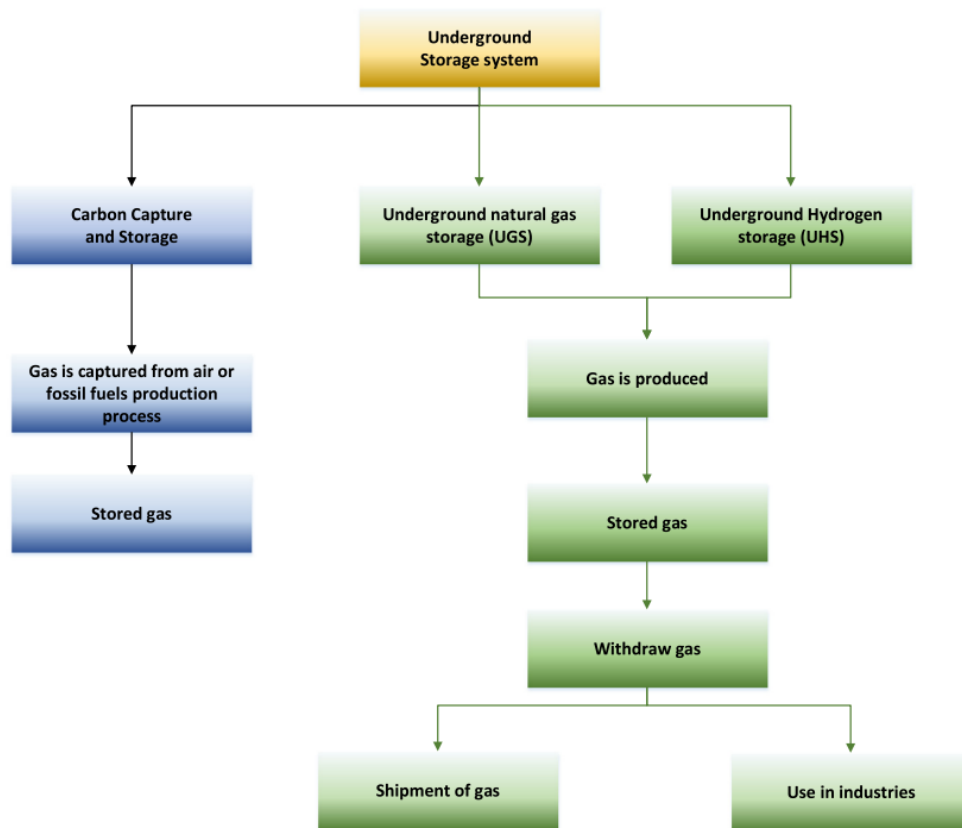


Figure 1—Purpose of underground storage system (USS) (Al-Shafi et al. 2023).

Previous studies have highlighted the operational challenges associated with hydrates in UGS reservoirs, emphasizing the need for effective mitigation strategies. Chemical inhibitors, thermal methods, and depressurization techniques are among the potential strategies to prevent and manage hydrate-related challenges in depleted wells. These strategies need to be tailored to the unique conditions of depleted wells to ensure their effectiveness and efficiency (Vrålstad et al. 2018). In addition to mitigation strategies, continuous monitoring and advanced reservoir management techniques are vital for detecting and addressing hydrate-related issues in real-time. Advanced monitoring technologies, such as downhole sensors and surveillance systems, offer valuable insights into reservoir conditions, enabling timely intervention to prevent or manage hydrate formation.

Storing gases underground is an effective way to manage excess renewable energy, allowing for reserves that can be used when demand outstrips supply. When geological conditions are unsuitable for underground storage, large-scale above ground containment becomes necessary. However, comparing these options reveals regional differences in renewable electricity-based energy systems (Elberry et al. 2021a). With technological advancements, hydrogen storage has become a viable method for seasonal storage, making it crucial to fully exploit the integration of variable renewable energy sources (VRES) into the grid (Elberry et al. 2021b). **Figure 2** shows underground natural gas storage.

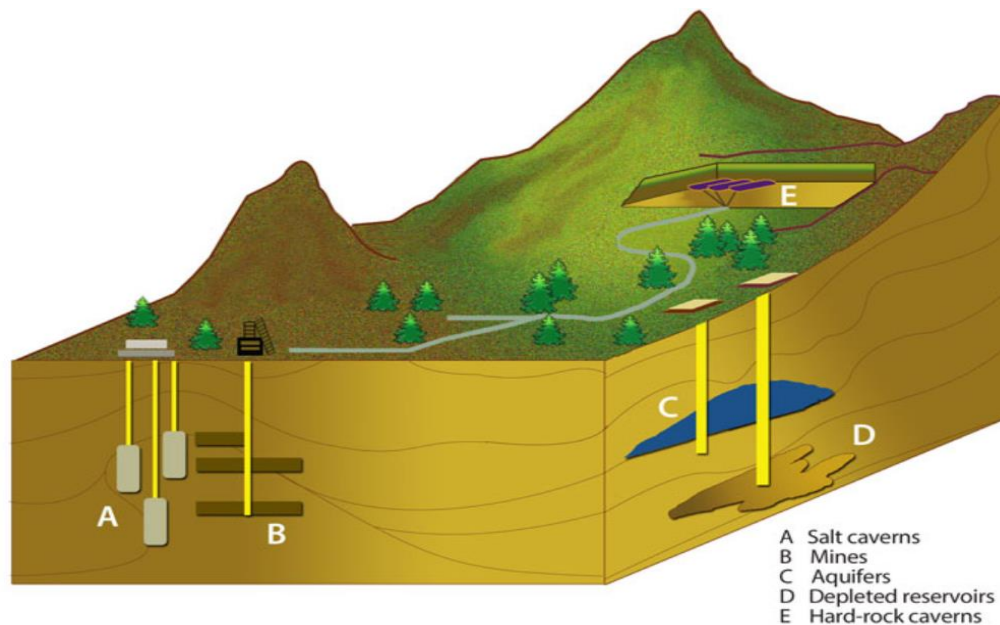


Figure 2—Underground natural gas storage (Energy Information Administration 2015).

Several volumetric metrics are used to define the core characteristics of an underground storage facility and the gas it holds. It's essential to differentiate between facility attributes, like capacity, and gas attributes, like actual inventory levels. These metrics include:

1. Total gas storage capacity: This is the maximum volume of gas that an underground storage facility can hold, considering its design, physical characteristics of the reservoir, installed equipment, and site-specific operating procedures.
2. Total gas in storage: This refers to the volume of gas stored in the facility at a given time.
3. Base gas (or cushion gas): This is the volume of gas kept as a permanent inventory in a storage reservoir to maintain adequate pressure and deliverability rates during the withdrawal season.
4. Working gas capacity: This is the total gas storage capacity minus the base gas.
5. Working gas: This is the volume of gas in the reservoir above the base gas level and is available for use in the market.
6. Deliverability: Often expressed in millions of cubic feet per day, this measure indicates the amount of gas that can be withdrawn from a storage facility daily. It can also be expressed in dekatherms per day (a therm is 100,000 Btu, approximately equal to 100 cubic feet of natural gas; a dekatherm is about one thousand cubic feet). Deliverability varies with the gas amount in the reservoir, reservoir pressure, compression capability, surface facilities' configuration, and other factors. Generally, the deliverability rate is highest when the reservoir is full and decreases as working gas is withdrawn.
7. Injection capacity (or rate): This is the daily amount of gas that can be injected into a storage facility, usually expressed in MMcf/day or dekatherms/day. Injection capacity depends on factors similar to those affecting

deliverability. However, the injection rate inversely varies with the total gas amount in storage. It is lowest when the reservoir is full and increases as working gas is withdrawn.

None of these measures for any given storage facility are fixed or absolute. **Table 1** summarizes and compares the mechanisms, strengths, limitations, and applications of various hydrate prediction models.

Table 1—Hydrate prediction model.

Model	Mechanism	Strength	Limitation	Applicability
Thermodynamic Model	These models predict the pressure and temperature conditions at which hydrates will form in a gas mixture (Bhatnagar and Gao 2022). They rely on thermodynamic equilibrium principles and utilize equations of state to describe the behavior of gas and water components within the system.	Thermodynamic equilibrium models are computationally efficient and provide a basic framework for hydrate formation prediction.	These models assume a system at equilibrium, which may not always be the case in real-world UGS scenarios with dynamic pressure and temperature conditions. Additionally, they may not account for the complex interactions between the reservoir rock and the gas-water mixture.	While these models offer a starting point for hydrate prediction in depleted wells, their limitations necessitate using them in conjunction with other methods for a more accurate assessment.
Kinetic Models	These models consider the kinetics of hydrate formation, accounting for the rate at which gas molecules are incorporated into the hydrate structure (Aghajanloo et al. 2024). They involve complex mathematical equations that describe mass transfer, heat transfer, and the surface chemistry involved in hydrate formation.	Kinetic models provide a more realistic picture of hydrate formation by incorporating reaction rates and non-equilibrium conditions. This can be particularly valuable in depleted well UGS where pressure and temperature fluctuations might occur.	Kinetic models are computationally expensive and require a deeper understanding of the specific reservoir characteristics and gas composition. Additionally, validating these models with real-field data can be challenging.	Kinetic models offer a more accurate prediction of hydrate formation risk in depleted wells compared to equilibrium models. However, their complexity and data requirements necessitate careful evaluation before implementation.
Pore-Scale Network Models	These models represent the pore space within the reservoir rock as a network of interconnected channels (Makwashi and Ahmed 2021). They simulate the flow of gas, water, and heat through this network, allowing for a detailed analysis of hydrate formation within the reservoir rock itself.	Pore-scale network models offer valuable insights into the spatial distribution of hydrates within the reservoir and their impact on flow behavior. This can be crucial for optimizing wellbore placement and production strategies in depleted wells.	These models are computationally very demanding and require detailed information about the pore structure of the reservoir rock, which can be challenging to obtain. Additionally, their complexity makes them less suitable for real-time decision making.	Pore-scale network models can be valuable tools for understanding hydrate formation processes in depleted wells. However, their computational intensity and data demands limit their widespread use in practical applications.

Methodology

Software Suite. MATLAB (version 2024) software suite was employed in this study for coding of the numerical problem. MATLAB was used to simulate the effect of hydrate in a gas well. Microsoft Office Excel (2013) software suite was used in this study for the collation and plotting of simulation results.

Data Collection. The data used for this study was collected from open sources (Guo et al. 2007) and are as defined in **Table 2**.

Table 2—Input data for a gas storage well.

Input Parameter	Value	Units
Gas gravity, γ_g	0.71	–
Tubing inside diameter, d_i	2.259	inch
Tubing relative roughness, ϵ/d_i	0.0006	–
Measured depth at tubing shoe, L	10,000	feet
Inclination angle, θ	0	degree
Wellhead pressure, p_{hf}	800	psia
Wellhead temperature, T_{hf}	150	°F
Bottom-hole temperature, T_{wf}	200	°F
Reservoir Pressure, p_r	2000	psia
c-constant in back-pressure IPR model, c	0.01	$Mscf/d - psi^{2n}$
n-exponent in back-pressure IPR model, n	0.8	–

Governing Equations. The governing equations for this study are the inflow performance relationship (IPR) and tubing performance relationship (TPR) for a gas well as given in **Eq. 1** and **2**, respectively (Guo et al. 2017), as follows,

$$q_{sc} = c(p_r^2 - p_{wf}^2)^n, \dots\dots\dots(1)$$

$$p_{wf}^2 = e^s p_{hf}^2 + \frac{6.67 \times 10^{-4} (e^s - 1) f_M Z_{av}^2 T_{av}^2 q_{sc}^2}{d_i^5 \cos \theta}, \dots\dots\dots(2)$$

where q_{sc} is the gas flow rate, c is the c-constant in IPR model, p_r is the reservoir pressure, p_{wf} is the flowing bottom-hole pressure, n is the n-exponent in the IPR model, s is the skin factor, f_M is the friction factor, Z_{av} is the average gas compressibility factor, T_{av} is the average temperature, d_i is the internal tubing diameter, and θ is the pipe angle of inclination.

Model Development. The effect of hydrate on the deliverability of a storage gas reservoir can be investigated by considering a well as shown in **Figure 3**. The flow involves simultaneous flow of gas, water, and hydrates. As shown, some of the hydrates are deposited on the pipes inner walls resulting in a decrease in the flow area. Hence, in this study we used the thickness of the hydrate film for this investigation. That is; the thickness of the hydrate film was increased from 0.0 inch through 1.0 inch and its effect on the deliverability examined.

First, we computed the inflow performance relationship (IPR) flowing bottom-hole pressure for the gas storage well as a function of flow rate. This was achieved by rearranging **Eq. 1** into **Eq. 3**.

$$p_{wf} = \sqrt[2]{p_r^2 - \left(\frac{q_{sc}}{c}\right)^{\frac{1}{n}}}, \dots\dots\dots(3)$$

where r_h is the inner radius of the hydrate film, r_i is the inner radius of the pipe, and d_h is the thickness of the hydrate film.

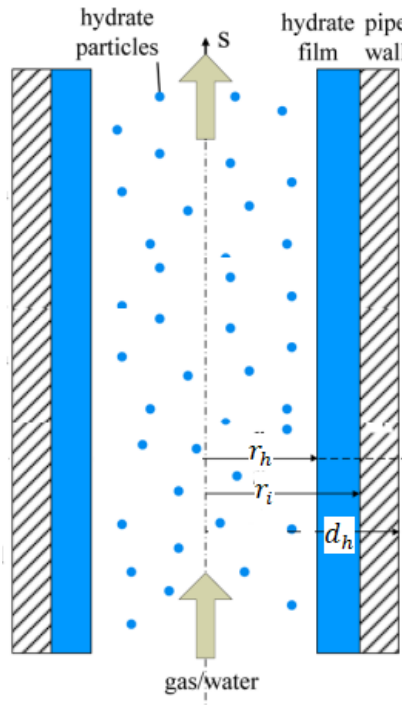


Figure 3—Multiphase gas-water-hydrate flow in a vertical well.

Second, the thickness of the hydrate film is modeled into the TPR model. This is achieved by the removing the hydrate thickness from the inner pipe diameter. We also assumed that the hydrate thickness in the pipe is constant. As shown in **Figure 3**,

$$r_h = r_i - \delta_h \dots \dots \dots (4)$$

In terms of diameter, **Eq. 4** can be rewritten as:

$$d_h = d_i - 2\delta_h \dots \dots \dots (5)$$

Equation defines the area for multiphase flow of the gas-water-hydrate multiphase flow. Notice that $d_h = d_i$ for $\delta_h = 0.0$.

We modified **Eq. 2** by introducing the effect of the film thickness, δ_h on the TPR equation with the aid of **Eq. 5**. That is

$$p_{wf} = \sqrt{e^S p_{hf}^2 + \frac{6.67 \cdot 10^{-4} (e^S - 1) f_M Z_{av}^2 T_{av}^2 q_{sc}^2}{(d_i - 2\delta_h)^5 \cos \theta}} \dots \dots \dots (6)$$

Eq. 6 is used in computing the TPR for the hydrate film thickness 0.0 inch through 1.0 inch. The average temperature and compressibility factor method was employed in this study. We also employed the bottom-hole pressure as the solution node.

Solution Procedure. In this section, we will describe the solution procedure employed in computing the IPR and TPR.

Average Temperature and Pressure. The first step was the computation of the average temperature and average pressure with the aid of **Eqs. 7** and **8**, respectively.

$$T_{av} = \left(\frac{T_{hf} + T_{wf}}{2} \right) + 460, \dots \dots \dots (7)$$

$$p_{av} = \left(\frac{p_{hf} + p_r}{2} \right) \dots \dots \dots (8)$$

Critical Temperature and Pressure. The second step is the computation of the critical temperature and critical pressure of the gas as functions of the gas gravity as defined in **Eqs. 9** and **10**, respectively.

$$T_{pc} = 168 + 325\gamma_g - 12.5\gamma_g^2, \dots \dots \dots (9)$$

$$p_{pc} = 667 + 15\gamma_g - 37.5\gamma_g^2 \dots \dots \dots (10)$$

Pseudo-Reduced Temperature and Pressure. The third step is the computation of the pseudo-reduced temperature and pressure with the aid of **Eqs. 11** and **12**, respectively.

$$T_{pr} = \frac{T_{av}}{T_{pc}}, \dots \dots \dots (11)$$

$$p_{pr} = \frac{p_{av}}{p_{pc}} \dots \dots \dots (12)$$

Average Compressibility Factor. The fourth step is the computation of the average z-factor with the aid of the (Brill and Beggs 1974) z-factor correlation.

$$Z_{av} = A + \left(\frac{1-A}{e^B} \right) + Cp_{pr}^D, \dots \dots \dots (13)$$

where

$$A = 1.39(T_{pr} - 0.92)^{0.5} - 0.36T_{pr} - 0.10, \dots \dots \dots (14)$$

$$C = 0.132 - 0.32 \log(T_{pr}), \dots \dots \dots (15)$$

$$E = 9(T_{pr} - 1), \dots \dots \dots (16)$$

$$F = 0.3106 - 0.49T_{pr} + 0.1824T_{pr}^2, \dots \dots \dots (17)$$

$$D = 10^F, \dots \dots \dots (18)$$

$$B = (0.62 - 0.23T_{pr})p_{pr} + \left(\frac{0.066}{T_{pr}} - 0.037 \right) p_{pr}^2 + \frac{0.32p_{pr}^6}{10^E} \dots \dots \dots (19)$$

Skin Factor and Skin Factor Exponent. The fifth step is the computation of the skin factor and the skin factor exponent as defined in **Eqs. 20** and **21**, respectively.

$$s = \frac{0.0375\gamma_g L \cos\left(\frac{\theta}{57.3}\right)}{Z_{av}T_{av}}, \dots \dots \dots (20)$$

$$e^s = \exp(s) \dots \dots \dots (21)$$

Friction Factor. The sixth step is the computation of the friction factor with the aid of the Nikuradse friction factor correlation (Guo et al. 2007) for fully turbulent flow in rough pipes as defined in **Eq. 22**,

$$f_M = \left(\frac{1}{1.74 - 2 \log\left(\frac{2\varepsilon}{d_i}\right)} \right)^2, \dots \dots \dots (22)$$

Absolute Open Flow. The seventh step is the computation of the absolute open flow or maximum flow rate with the aid of Eq. 1 @ $p_{wf} = 0$,

$$q_{sc} = cp_r^{2n} \dots \dots \dots (23)$$

Gas Flow Rate Generation. The eight step is the generation of gas flow rate in the range from zero to absolute open flow in steps of AOF divided by 14 as defined in **Eq. 24**.

$$q_{sc} = 0 : AOF/14 : AOF \dots \dots \dots (24)$$

Inflow Performance Relationship. The ninth step is the computation of the inflow performance relationship for generated gas flow rates as defined in **Eq. 25**.

$$IPR(i) = \sqrt{p_r^2 - \left(\frac{q_{sc}(i)}{c}\right)^{\frac{1}{n}}} \dots \dots \dots (25)$$

Tubing Performance Relationship. The tenth step is the computation of the tubing performance relationship for the generated gas flow rates and the different hydrate film thickness as defined in **Eq. 26**.

$$TPR(i) = \sqrt{e^s p_{hf}^2 + \frac{6.67 \cdot 10^{-4} (e^s - 1) f_M Z_{av}^2 T_{av}^2 q_{sc}^2(i)}{(d_i - 2\delta_h)^5 \cos \theta}} \dots \dots \dots (26)$$

Gas Well Deliverability. The deliverability of the gas well is investigated by plotting the IPR and the TPRs obtained for the different hydrate film thickness. The point of intersection of the IPR and the various TPRs corresponds to the operating flow rate and operating pressure of the gas well. These operating flow rates and operating pressures are extracted and plotted against the corresponding hydrate film thickness. These plots will provide information on the effect of hydrates on gas well deliverability.

Result and Discussion

Figure 4 shows a plot of the IPR and TPR for the gas well as defined in Table 2 for the hydrate film thickness range as defined in **Table 3**. As shown the TPR is almost horizontal for zero hydrate film thickness and starts to curve upwards as the film thickness increases to almost vertical for 1.0 hydrate film thickness. It is also evident that the operating point changes as the hydrate film thickness increases.

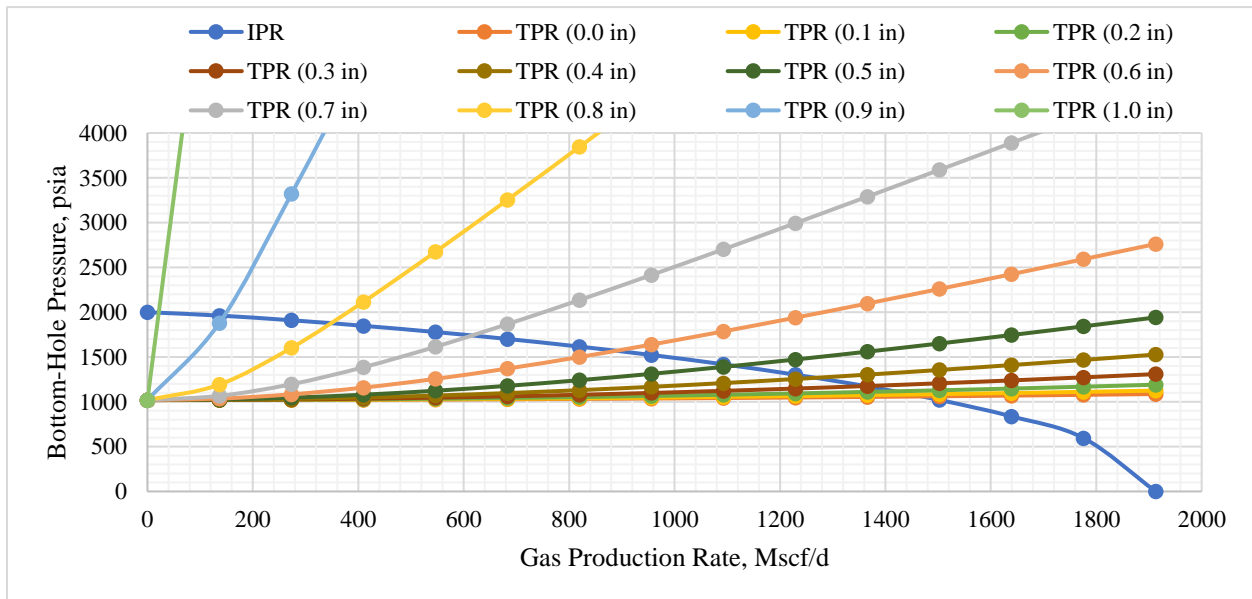


Figure 4—Nodal Analysis for varying hydrate film thickness.

Table 3—Hydrate film thickness range.

	Min	Max	Units
Hydrate Film Thickness	0.0	1.0	inch

Figure 5 shows a plot of the hydrate film thickness as a function of the operating gas flow rate. It is evident in Figure 5 that the operating rate decreases with increase in the hydrate film thickness. In fact, the operating flow rate is 1470 Mscf/day for zero hydrate film thickness and 20 Mscf/day for 1.0 inch hydrate film thickness. This is a clear indication that hydrate deposition on the pipeline walls will result in poor deliverability and may even result in no flow at the surface.

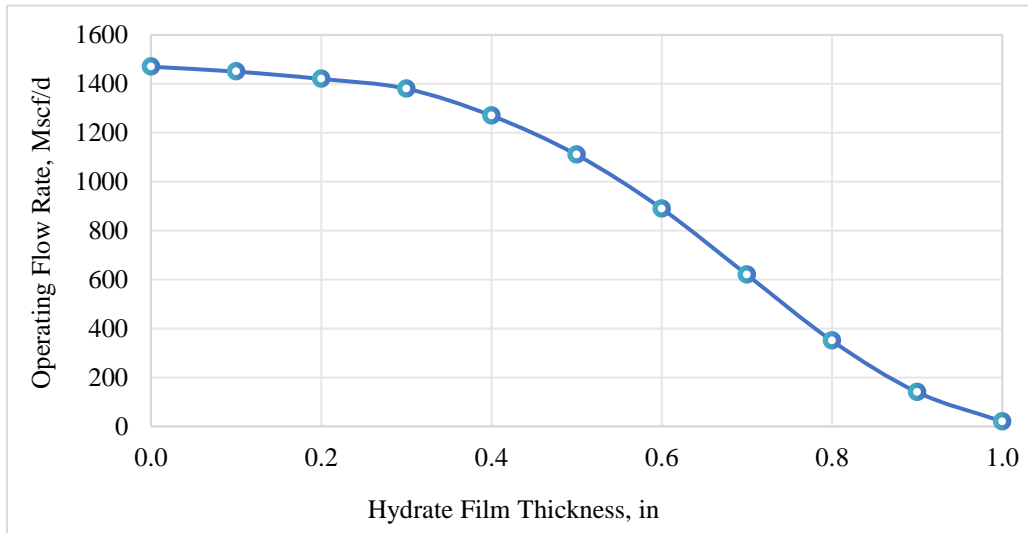


Figure 5—Effect of hydrate film thickness on gas well operating flow rate.

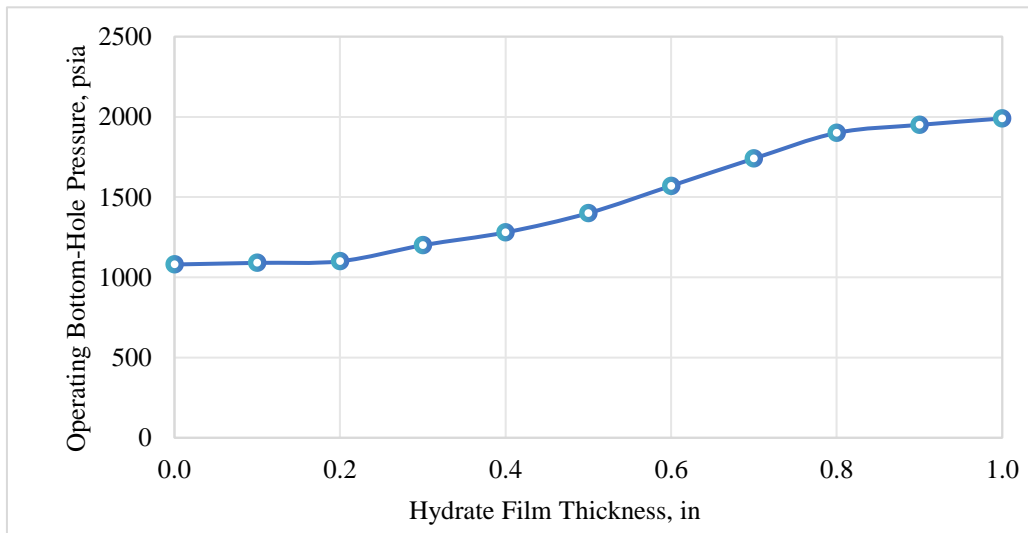


Figure 6—Effect of hydrate film thickness on gas well operating pressure.

Figure 6 shows a plot of the hydrate film thickness as a function of the operating bottom-hole pressure. It is evident that the operating bottom-hole pressure increases with increase in the hydrate film thickness. The operating pressure at zero hydrate film thickness is 1080 psia which translates to a drawdown of 920 psia. This drawdown pressure will be able to lift the gas at a flow rate of 1470 Mscf/day (Figure 5). However, the operating

pressure at 1.0 inch hydrate film thickness is 1990 psia with a drawdown of 10 psia which is not enough to lift the gas and the well will die. Hence, the effect of gas hydrate is to reduce gas well deliverability.

Conclusions

This study investigated the effect of hydrate on undergraduate gas storage deliverability. The following conclusions are drawn from the results and discussion presented in this study.

1. Nodal analysis revealed that the TPR curves upward from horizontal for a case with no hydrate film to vertical upward for cases with increasing hydrate film thickness.
2. The results also revealed that the operating gas flow rate decreases with increase in hydrate film thickness which is an indication that hydrate results in poor gas deliverability.
3. The operating bottom-hole pressure increases with increase in hydrate thickness which translates into a decrease in draw down and hence poor gas deliverability.
4. High hydrate deposition will kill the well evident in the operating flow rate of 20 Mscf/day for hydrate film thickness of 1.0 inch.

Recommendations

The following recommendations are suggested:

1. Hydrate inhibitors should be introduced in gas wells to prevent the formation of hydrates which when deposited will result to poor well deliverability.
2. The pipes should be insulated to prevent heat loss to the environment that will promote hydrate formation once temperature drops below the hydrate formation temperature.

Conflicting Interests

The author(s) declare that they have no conflicting interests.

Reference

- Aghajanloo, M., Yan, L., Berg, S., et al. 2024. Impact of CO₂ Hydrates on Injectivity during CO₂ Storage in Depleted Gas Fields: A Literature Review. *Gas Science and Engineering* **123**:205250.
- Al-Shafi, M., Massarweh, O., Abushaikha A. S., Bicer Y. 2023. A Review on Underground Gas Storage Systems: Natural Gas, Hydrogen and Carbon Sequestration. *Energy Reports* **9**(1): 6251-6266.
- Bhatnagar, G. and Gao, S. 2022. Gas hydrate management. In *Oil and Gas Chemistry Management Series, Flow Assurance*. Chap. 1, 1-50. Amsterdam: Gulf Professional Publishing.
- Brill, J. P. and Beggs, H. D. 1974. Two-Phase Flow in Pipes, University of Tulsa. INTERCOMP Course, The Hague.
- Chu, H., Zhang, J., Li, J., et al. 2023. Impact of Well Interference on Transient Pressure Behavior During Underground Gas Storage: A Comparative Study. Paper presented at the SPE Annual Technical Conference and Exhibition, San Antonio, Texas, USA, 9-11 October. SPE-214780-MS.
- Dillon, W. P. 2002. Gas Hydrate in the Ocean Environment. In *Encyclopedia of Physical Science and Technology* (Third Edition): 473-486.
- Energy Information Administration (EIA). 2015. The Basics of Underground Natural Gas Storage. <https://www.eia.gov/naturalgas/storage/basics/> (accessed 1 September 2024).
- Elberry, A. M., Thakur, J., Santasalo-Aarnio, et al. 2021a. Large-scale Compressed Hydrogen Storage as Part of Renewable Electricity Storage Systems. *Int. J. Hydrog. Energy* **46**(29): 15671-15690.
- Elberry, A. M., Thakur, J., and Veysey, J. 2021b. Seasonal hydrogen Storage for Sustainable Renewable Energy Integration in the Electricity Sector: A Case Study of Finland. *J. Energy Storage* **44**(1):103474.
- Guo, B., Liu, X., and Tan, X. 2017. *Petroleum Production Engineering*, second edition. Amsterdam: Gulf Professional Publishing.

- Guo, B., Lyons, W. C., and Ghalambor, A. 2007. *Petroleum Production Engineering: A Computer-Assisted Approach*. Amsterdam: Gulf Professional Publishing.
- Makwashi, N. and Ahmed, T. 2021. Gas Hydrate Formation: Impact on Oil and Gas Production and Prevention Strategies. *6*(1): 61-75.
- Muhammed, N., Bashirul, H., Shehri, D., et al. 2023. Hydrogen Storage in Depleted Gas Reservoirs: A Comprehensive Review. *Fuel* **337**(1): 127032.
- Vrålstad, T., Saasen, A., Fjær, E., et al. 2018. Plug and Abandonment of Offshore Wells: Ensuring Long-Term Well Integrity and Cost-Efficiency. *Journal of Petroleum Science and Engineering* **173**(1):251-270.
- Wang, X. and Economides, M. 2009. *Advanced Natural Gas Engineering*, 115-169. Amsterdam: Gulf Publishing Company.

Dr. Charlie Iyke Anyadiegwu is a Senior Lecturer in the Department of Petroleum Engineering, Federal University of Technology Owerri where he has worked for over 25 years. He holds both B. Eng and M. Eng in Petroleum Engineering and Gas Engineering Respectively from the University of Portharcourt, Rivers State, Nigeria, and Ph.D. in Petroleum Engineering from the Federal University of Technology Owerri, Nigeria. His research interests are in oil and gas production and processing from fossil fuel and non-fossil fuel (Biomass), health, safety and environment (HSE), oil spillage detection, control and prevention.

Christian Emelu Okalla is a Technologist and Researcher at the Department of Petroleum Engineering, Federal University of Technology Owerri, Nigeria. He holds both B. Eng and M. Eng in Petroleum Engineering from the Federal University of Technology Owerri. His research interests are in drilling engineering, production engineering, natural gas engineering, reservoir engineering, and reservoir simulation.

Dr. Anthony Kerunwa is a Senior Lecturer in the Department of Petroleum Engineering, Federal University of Technology Owerri, Nigeria. He holds both B. Eng and M. Eng in Petroleum Engineering from the Federal University of Technology Owerri, and Ph.D in Petroleum Engineering from Centre for Oil field Chemical Research (IPS). His research interests are in drilling engineering, production engineering, reservoir engineering, petroleum economics.

Nmesoma Precious Ebosie is a recent graduate of the Department of Petroleum Engineering, Federal University of Technology Owerri, Nigeria. She holds a B. Eng in Petroleum Engineering from the Federal University of Technology Owerri. Her research interests are in drilling engineering, production engineering, and reservoir engineering.

Daniel Chinedu Nwachukwu is a recent graduate of the Department of Petroleum Engineering, Federal University of Technology Owerri, Nigeria. He holds a B.Eng in Petroleum Engineering from the Federal University of Technology Owerri. His research interests are in drilling engineering, production engineering, and reservoir engineering.